Physics of the Coefficient of Friction in CMP

Len Borucki[a], Ara Philipossian, and Yun Zhuang
Araca, Inc., 6655 North Canyon Crest Drive, Suite 1205, Tucson AZ 85750, USA

[a]E-mail : Len.Borucki@gmail.com

(Received May 8 2006, Accepted August 18 2006)

The implications of a theory of lubricated pad asperity wafer contact are traced through several fundamental areas of chemical-mechanical polishing. The hypothesized existence of a nanolubrication layer underlies a high accuracy model of polish rates. It also provides a quantitative explanation of a power law relationship between the coefficient of friction and a measure of pad surface flattening. The theory may further be useful for interpreting friction changes during polishing, and may explain why the coefficient of friction is sometimes observed to have a temperature or velocity dependence.

Keywords : Friction, Lubrication, Chemical-mechanical polishing

1. INTRODUCTION

The problem of understanding the physics and of developing models for chemical-mechanical planarization (CMP) processes has progressed considerably since the empirical removal rate model of Preston[1]. Runnels[2], for example, pointed out the potential importance of hydrodynamics. Many individual pieces of the physics for polishing silicon dioxide and copper on a rotary tool using commercially available slurries and polymeric pads are well-enough developed to make useful predictions. For example, abstract two-step removal rate models involving both mechanical and chemical rates describe blanket removal in some systems within the repeatability of measurements[3,4], often with RMS errors of 50 A/min or less (Fig. 1). This makes such models useful for prediction of rates at pressures and velocities that may be required for future processes and for understanding rate changes related to wafer and tool scaling[5]. A key part of achieving this level of accuracy is a model for the chemical reaction temperature[3]. In CMP, the directly measurable temperatures of the pad, wafer and slurry, all of which can be modeled in detail[6,7], do not seem able to high enough to produce the chemical rates required in silicon dioxide polishing[8], although they might be close to correct for copper polishing[4]. The required reaction temperatures for oxide, however, might be reachable as a result of localized flash heating during *lubricated* sliding contact between sufficiently tall asperities and the wafer[3]. Finite element simulations of lubricated flash heating also predict a power law dependence of heat partitioning to the pad on sliding velocity, one of the key elements of the compact two step removal rate model in[3]. The same simulations indicate that the lubrication layer thickness and the pad topography are critical. Topography due to conditioning can be modeled[9] and related to changes in oxide polish rates over time by linking the conditioning model to the two-step chemical-mechanical model[10]. For oxide, the critical link between chemical and mechanical rates and topography seems to come about via the coefficient of friction (COF), which empirically is found to be negatively correlated with a surface measure called the pad flatness ratio, or PFR[10] (Fig. 2). The PFR measures that fraction of light incident on an unloaded pad sample that is reflected directly back to the light source. The PFR is low when the surface is rough and high when asperities have been substantially flattened by wafer-induced processes.

It is generally agreed now that most of the physics responsible for removal in boundary lubrication mode occurs at or near microscopic pad asperity contacts. Models of microscopic contact have focused largely on static three body mechanical interaction between asperity tips, slurry particles, and the wafer surface[11,12]. Some models have also considered the possibility of a very thin nanometer scale lubrication layer between asperity tips and the wafer surface, a key part of our removal rate model. The existence of such a layer may provide an explanation for why rates can sometimes be observed to rise and than fall again as the mean slurry particle size increases[13]. Evidently, the peak in rate comes about due to sampling of different parts of the slurry particle size distribution by the nanolubrication layer[14], with the highest rate occurring when the mean layer thickness is on the order of the mean particle size.

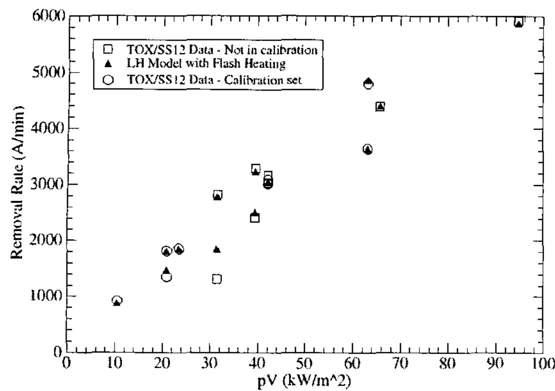

Fig. 1. High accuracy fit (RMS error 52 A/min) and prediction of thermal oxide polishing data[3].

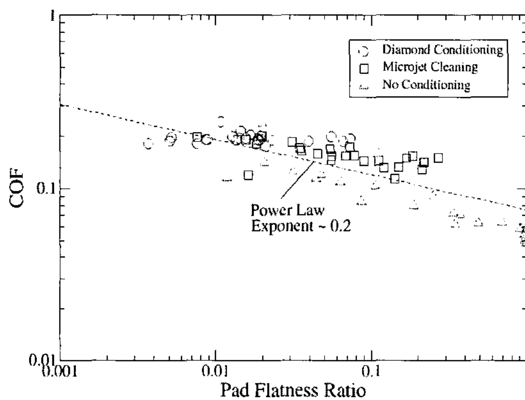

Fig. 2. Coefficient of friction vs. pad flatness ratio[10].

In this paper, we examine another implication of the nanolubrication idea. We will argue that the existence of such a layer may provide an explanation of the correlation between the coefficient of friction and the PFR if PFR is interpreted as measuring asperity tip curvature. It may also elucidate why the COF can depend on temperature and on velocity in the boundary lubrication regime.

2. ELASTOHYDRODYNAMIC LUBRICATION

Elastohydronamic lubrication (EHL) theory has long been applied to bearing design, where it is used to estimate the minimum lubrication layer thickness. In addition to the load and sliding speed, there are two important physical factors that determine the lubrication layer thickness: the elasticity of the slider (an asperity in the case of CMP), and the pressure dependence of the fluid viscosity. Over the normal range of CMP real asperity contact pressures, changes in fluid viscosity

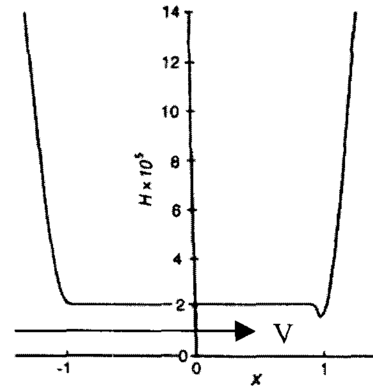

Fig. 3. Cross section of a lubricated elastic line contact at steady state[15].

occur but are not of the same magnitude as in lubricating oils. Thus we will ignore pressure-induced viscosity changes here for simplicity. The lubrication problem then involves a coupled system involving the isoviscous Reynolds equation for the fluid flow and the elasticity equations for asperity deformation. Two geometries have been extensively analyzed: the line contact and the point contact. At steady state, the theory predicts that a thin film of nearly constant thickness h_c will form under a line contact except for a slight restriction at the trailing edge (Fig. 3). For the point contact, which has a circular contact area, something similar happens except that an approximately rectangular region of nearly constant fluid thickness forms that is bounded laterally and at the trailing edge by flow restrictions. In real pad materials, the contact geometry is not so idealized. Muldowney[16], used confocal microscopy to image actual dry loaded contact shapes for IC1000^{TM} and found that they often have a crescent shape due to conditioning of the walls between spherical voids in the pad. Thus, an analysis based on an ideal contact shape is likely to be very approximate.

One of the predictions of EHL theory is that the deformed contact area is nearly the same as in dry contact. The fluid pressure in the lubrication layer is also positive and can therefore support the applied load. For circular contacts, the pressure distribution is approximately the same as the distribution from dry Hertzian contact theory[17]. From extensive numerical simulations, compact design formulas have been produced for the minimum fluid thickness and the thickness h_c in the constant central region. For an elastic isoviscous nominal point contact, h_c is approximately [18]

$$h_c(\delta) \approx 2.34 \cdot (\mu_0 V(1-\nu^2)/E)^{0.64} R^{0.69} \delta^{-0.33} \quad (1)$$

where μ_0 is the viscosity, V is the sliding speed, R is the undeformed asperity tip radius of curvature, ν is the pad

Poisson ratio, E is Young's modulus, and δ is the tip displacement. Since the contact area in Hertzian contact theory is $A_c = \pi R\delta$ [17], it follows from Eqn. (1) by eliminating R that h_c increases with the contact area and the velocity and decreases with the applied load, which determines δ. We note that elevated temperatures affect h_c through both μ_0 and E.

3. THE COEFFICIENT OF FRICTION

Removal rates have a direct relationship to the coefficient of friction because both the mechanical shear force and the temperature rise above ambient are proportional to the COF. Contributions to the total shear force measured on a tribometer include mechanical shear forces from three body sliding contact and viscous shear forces. Wafer scale hydrodynamic pressures under the wafer can also affect the measured shear force, but these are generally absent in concentrically grooved pads. Here, we analyze the viscous shear force, which is small over most of the wafer surface but may be locally large in a nanolubrication layer.

Neglecting pressure gradient contributions, which can be shown to be small, the viscous shear stress is approximately

$$\tau = \frac{\mu_0 V}{h} \tag{2}$$

where h is the local fluid thickness. The total contribution to the COF from the viscous shear force F_{visc} is then

$$\mu_{visc} = \frac{F_{visc}}{F} \approx \frac{1}{pA}\iint_A \frac{\mu_0 V}{h} dA \approx \frac{\mu_0 V}{pA}\sum_i \frac{A_i}{h_i} \tag{3}$$

where p is the nominal applied wafer pressure, A is the wafer area, $F=pA$ is the total load, A_i is the area of the ith asperity contact, and h_i is the nanolubrication layer thickness of the ith contact. The first integral in Eqn. (3) is taken over the entire wafer surface while the sum is over only the asperity contact areas. These expressions are approximately equal because the viscous shear force drops off rapidly away from the contact area when the asperity sides are sufficiently steep. By using a single fluid layer thickness for each asperity, we are also invoking the EHL result that the lubrication layer thickness is nearly constant.

We now relate the sum in Eqn. (3) to the asperity summit height distribution. If there are N asperities under the wafer with area density $\eta = N/A$ and $\phi(z)$ is the summit height probability density distribution, then the number with height between z and $z+dz$ is $N\phi(z)dz$. If the wafer is at height d, then neglecting wafer tilt, all of these asperities will have the same Hertzian contact area $\pi R(z-d)$ and the same nanolubrication layer thickness $h_c(z-d)$ provided that they have the same tip curvature. We will adopt this latter assumption throughout. Thus, we may group terms in the sum in Eqn. (3) by undeformed summit height z_i and write the sum as

$$\sum_i \frac{A_i}{h_i} = \sum_i \frac{\pi R(z_i - d)}{h_c(z_i - d)} N\phi(z_i)dz \tag{4}$$

The sums in Eqn. (4) are only over asperities with heights z_i exceeding d. Finally, we replace the second sum in Eqn. (4) by an integral and combine the result with Eqn. (3) to obtain an estimate for the viscous contribution to the COF:

$$\mu_{visc} \approx \frac{\mu_0 V \eta \pi R}{p}\int_d^\infty \frac{z-d}{h_c(z-d)}\phi(z)dz \tag{5}$$

The wafer contact distance d in Eqn. (5) comes from load balance, which in the Greenwood and Williamson model [17] is given by

$$p = \frac{4E\eta R^{1/2}}{3(1-\nu^2)}\int_d^\infty (z-d)^{3/2}\phi(z)dz \tag{6}$$

An explicit expression for the viscous contribution to the COF can be worked out in the special case in which the summit height PDF has an exponential tail with decay length λ that includes the contract region, $\phi(z) = B\exp(-z/\lambda)$ for $z \ge z_0$ and $d \ge z_0$. Such tails are often observed in interferometry data. In this case, after some algebra, it can be shown by substituting Eqn. (1) into Eqn. (5), integrating, and applying Eqn. (6) to eliminate d that

$$\mu_{visc} \approx 0.9\cdot(\mu_0 V(1-\nu^2)/E)^{0.36} R^{-0.19} \lambda^{-0.17} \tag{7}$$

If we now interpret the PFR as being proportional to the mean asperity tip radius of curvature, $PFR \propto R$, then Eqn. (7) states that the viscous contribution to the COF should vary like $PFR^{-0.19}$. In fact we do find a power law relationship between the total COF and PFR with an exponent of about -0.2 (Fig. 2). The power law relationship is particularly clear when the COF is low due to the absence of conditioning.

Calculated values of μ_{visc} using Eqn. (7) are shown in Fig. 4 for a range of values of E and R using a value of λ=0.91 μm measured from an IC1000™ pad. A sliding

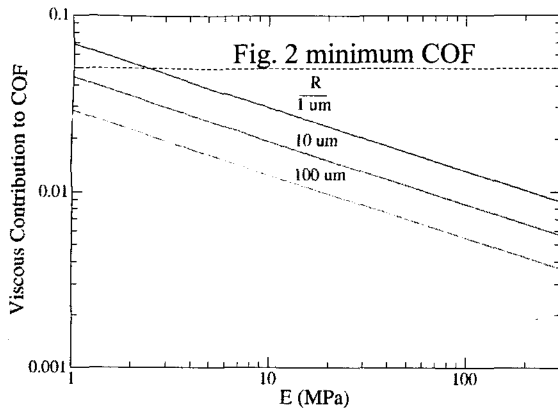

Fig. 4. Computed viscous contribution to the COF as a function of E and R.

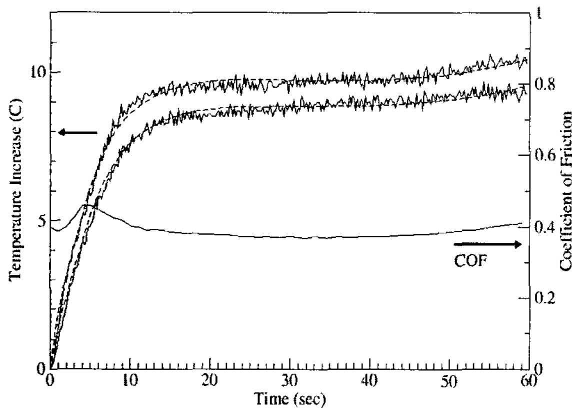

Fig. 5. Correlation of COF with temperature in an ILD polishing experiment[19].

velocity of 1 m/sec, room temperature slurry and a Poisson ratio of 0.5 were assumed in this figure. We see that μ_{visc} is smaller than the lowest COF (0.05) observed in the experiments in Fig. 2 except for E in the 1-10 MPa range and R below 10 μm. The low COF contribution predicted by this model may result in part from treating the contacts as idealized point contacts. Other possible sources of error may be the steady state assumption behind Eqn. (1) and the assumption of constant viscosity. Molecular dynamics simulations and thin film friction experiments indicate that large increases in viscosity occur when the lubricating layer is only a few monolayers thick[21].

Equation (7) also implies that thermal softening of the asperity tip should increase the viscous part of the COF by decreasing E. The viscous contribution to the COF may therefore not only be partially causative in creating a temperature increase but will also be affected by it. Observations of softening effects on COF are complicated by the fact that the viscosity of water decreases by more than a factor of three between room

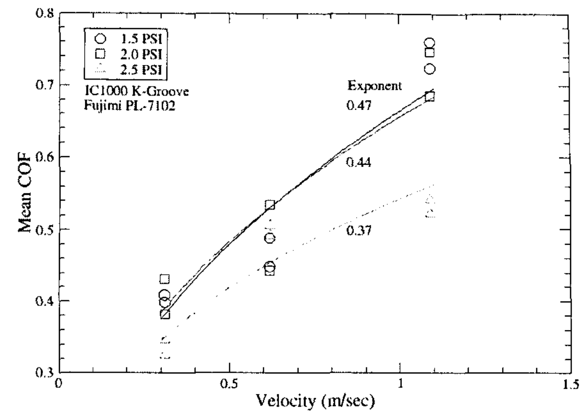

Fig. 6. Variation of COF with velocity in a copper polishing experiment[20].

temperature and the boiling point. In Fig. 5[19], for example, we show a correlation between COF and leading and trailing edge pad temperatures during a silicon dioxide polishing experiment. In light of Eqn. (7), one might interpret the increase in COF during the first four seconds of the temperature transient to asperity softening since all of the slurry on the pad is initially at room temperature. As the high heat capacity slurry warms up, however, the COF again drops as the viscosity decreases. At much longer times, softening again begins to dominate COF due to heat storage in the platen and polishing head.

Equation (7) also implies a power law dependence of COF on velocity. In Fig. 6, we show COFs that were measured during copper polishing as a function of velocity at several pressures[20]. The COF in this data approximately follows a power law with exponents consistent with Eqn. (7).

4. SUMMARY AND CONCLUSIONS

We have argued that an elastohydrodynamic nanolubrication layer is an important element in modeling and interpreting CMP process data. The hypothesized layer underlies a lubricated flash heating thermal model that is critical to high accuracy modeling of the pressure and velocity dependence of chemical rate variations in the polishing of silicon dioxide, copper and other metals. The existence of the layer may explain why removal rates do not always vary monotonically with particle size. The power law dependence of COF on PFR and the observed power law exponent are both predicted by the theory. Thermal dependence of the viscosity and pad modulus in the theory may help to explain variations in COF that are seen during polishing experiments. The

theory is also consistent with some observations that show a velocity dependence of COF in the boundary lubrication regime. A more accurate treatment of asperity shape, of the transient aspects of layer formation, and of the fluid layer thickness dependence of viscosity may lead to estimates of the magnitude of the viscous contribution to COF that are more in line with measurements. Finally, the action of particles should find an interesting place within the context of nanolubrication theory.

ACKNOWLEDGEMENTS

The authors would like to thank C.P. Please, T. Witelski, C. Breward, D. Schwendeman, M. Gratton, J. Evans, A. Bhattacharya, M. Nichols and M. Surles for stimulating discussions on the implications of nanolubrication at the 2005 Mathematical Problems in Industry workshop held at Worcester Polytechnic Institute on 13-17 June, 2005.

REFERENCES

[1] F. Preston, J. of the Society. of Glass Technology, Vol. 11, p. 214, 1927.
[2] S. R. Runnels, J. Electrochem. Soc., Vol. 141, No. 7, p. 1900, 1994.
[3] J. Sorooshian, L. Borucki, D. Stein. R. Timon, D. Hetherington, and A. Philipossian, Trans. ASME J. Tribology, Vol. 127, No. 3, p. 639, 2005.
[4] L. Borucki, J. Sorooshian, Z. Li, Y. Sampurno, Y. Zhuang, and A. Philipossian, Proc. 9th International CMP-MIC, Fremont, CA, p. 168, 2005.
[5] L. Borucki, D. Rosales-Yeomans, and A. Philipossian, Proc. 10th CAMP CMP Symposium, Lake Placid, NY, 2005.
[6] Y. Sampurno, L. Borucki, and A. Philipossian, J. Electrochem. Soc., Vol. 152, No. 11, 2005.
[7] G. P. Muldowney, Proc. Pac RIM-CMP Conference, Tokyo, Japan, p. 33, 2004.
[8] S. Gold and V. A. Burrows, Electrochem. and Solid State Letters, Vol. 7, No. 12, p. G295, 2004.
[9] L. J. Borucki, T. Witelski, C. P. Please, P. R. Kramer, and D. Schwendeman, J. Engineering Mathematics, Vol. 50, p. 1, 2004.
[10] L. Borucki, H. Lee, Y. Zhuang, and A. Philipossian, Proc. AIChE Annual Meeting, Austin TX, 2004.
[11] J. Luo and D. Dornfeld, IEEE Trans. on Semiconductor Manufacturing, Vol. 14, No. 2, p. 112, 2001.
[12] X. Xia and G. Ahmadi, Particulate Science and Technology, Vol. 20, No. 3, p. 187.
[13] C. Zhou, L. Shan. J. R. Hight, S.-H. Ng, and S. Danyluk, Mat. Res. Soc. Symp. Proc., Materials Research Society, San Francisco, CA, Vol. 671, p. M1.6.1, 2001.
[14] S.-H. Ng, doctoral dissertation, Georgia Institute of Technology, Atlanta, GA, 2004.
[15] A. Z. Szeri, Fluid Film Lubrication Theory and Design, Cambridge U. Press, Ch. 8, 1998.
[16] G. Muldowney, C. L. Elmufdi, and R. Palaparthi, Proc. 10th CAMP CMP Symposium, Lake Placid, NY, 2005.
[17] K. L. Johnson, Contact Mechanics, Cambridge U. Press, 1985.
[18] B. J. Hamrock and D. Dowson, Trans. ASME J. Lubrication Technology, Vol. 100, p. 236, 1978.
[19] L. Borucki, L. Charns, and A. Philipossian, J. of the Electrochemical Soc., Vol. 151, No. 12, p. G809, 2004.
[20] Z. Li, doctoral dissertation, the University of Arizona, Tucson, AZ, 2005.
[21] P. A. Thompson, G. S. Grest, and M. O. Robbins, "Phase transitions and universal dynamics in confined films," Phys. Rev. Lett., Vol. 68, p. 3448, 1992.